LANGMUIR

Article

pubs.acs.org/Langmuir

Complex Behavior of Aqueous α-Cyclodextrin Solutions. Interfacial Morphologies Resulting from Bulk Aggregation

Jorge Hernandez-Pascacio,[†] Ángel Piñeiro,[‡] Juan M. Ruso,[‡] Natalia Hassan,[‡,⊥] Richard A. Campbell,[*,§] José Campos-Terán,[*,∥] and Miguel Costas[*,†]

[†]Laboratorio de Biofisicoquímica, Departamento de Fisicoquímica, Facultad de Química, Universidad Nacional Autónoma de México, México D. F. 04510, Mexico

[‡]Soft Matter and Molecular Biophysics Group, Department of Applied Physics, University of Santiago de Compostela, Santiago de Compostela 15782, Spain

[§]Institut Laue-Langevin, 71 avenue des Martyrs, CS 20156, 38042 Grenoble, Cedex 9, France

[∥]Departamento de Procesos y Tecnología, Universidad Autónoma Metropolitana, Unidad Cuajimalpa, Av. Vasco de Quiroga 4871, Col. Santa Fe, Delegación Cuajimalpa de Morelos 05348, Mexico

Supporting Information

ABSTRACT: The spontaneous aggregation of α-cyclodextrin (α-CD) molecules in the bulk aqueous solution and the interactions of the resulting aggregates at the liquid/air interface have been studied at 283 K using a battery of techniques: transmission electron microscopy, dynamic light scattering, dynamic surface tensiometry, Brewster angle microscopy, neutron reflectometry, and ellipsometry. We show that α-CD molecules spontaneously form aggregates in the bulk that grow in size with time. These aggregates adsorb to the liquid/air interface with their size in the bulk determining the adsorption rate. The material that reaches the interface coalesces laterally to form two-dimensional domains on the micrometer scale with a layer thickness on the nanometer scale. These processes are affected by the ages of both the bulk and the interface. The interfacial layer formed is not in fast dynamic equilibrium with the subphase as the resulting morphology is locked in a kinetically trapped state. These results reveal a surprising complexity of the parallel physical processes taking place in the bulk and at the interface of what might have seemed initially like a simple system.

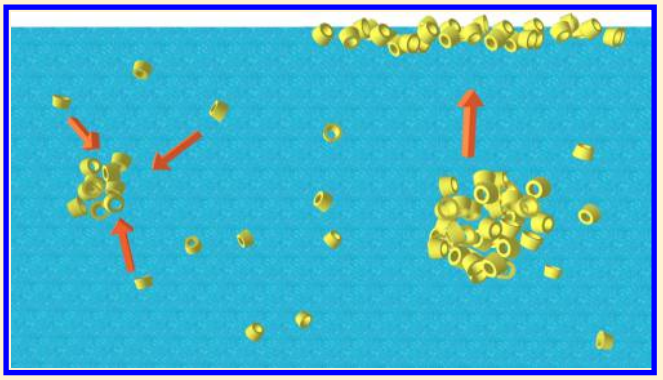

1. INTRODUCTION

Cyclodextrins (CDs) are cyclic oligosaccharides formed by six (α), seven (β), or eight (γ) 1,4-linked α-D-glucopyranoside units that result from the enzymatic degradation of starch. They have been described as truncated cone shaped molecules with both a hydrophobic cavity, which increases in size from α- to γ-CD, and a hydrophilic region located at their external surface. CDs are unique molecules from several points of view. They are probably the first family of molecules that springs to mind when looking for means to encapsulate small atomic groups of significant hydrophobicity. CDs meet a number of characteristics that are not easy to bring together in a family of compounds: low toxicity, biocompatibility, chemical stability, and ease of synthesis and purification.[1,2] Additionally, CDs are good targets for chemical modifications,[3] which on many occasions are able to enhance one or several of those characteristics.[4] Because of these general features, the number of basic studies and practical applications of CDs in several areas is very large. Nevertheless, the fundamental behavior of CDs in aqueous solutions is not fully understood.

There are two previous categories of experimental results for aqueous solutions of CDs that are particularly relevant to the present work. The first concerns the bulk aqueous solution where it was shown by Coleman et al. that α-, β-, and γ-CD exist in the form of aggregates bound together by a network of hydrogen bonds.[5] This study was followed up by González-Gaitano et al. and Puskas et al., who reported cyclodextrin molecules spontaneously form aggregates,[6,7] and while Valente et al. did not observe aggregates in α-CD, β-CD, and γ-CD solutions using NMR experiments, they commented that aggregates could be present at a concentration up to 1%.[8] The issue has been further discussed explicitly in two reviews.[9,10] The aggregation of CD molecules in the bulk solution is an important finding because recently it has been reported that CD aggregates contribute to the solubilization of poorly soluble drugs,[11] making this phenomenon very relevant

Received: April 29, 2016
Revised: June 8, 2016
Published: June 14, 2016

DOI: 10.1021/acs.langmuir.6b01646
Langmuir 2016, 32, 6682−6690

to the pharmaceutical industry. CDs have also been employed as a chemical reaction medium to favor the recovery of the reactants and products, thus preventing contamination.[12] The second category concerns the liquid/air interface. Some years ago, we showed that significant quantities of α-CD are present at the surface even though the surface tension is very close to that of pure water.[13,14] This surface was transferred to mica sheets using Langmuir−Blodgett deposition, and the resulting dried film was characterized using atomic force microscopy.[14] Also, we have reported recently a detailed computational study on the adsorption and aggregation of α-CD and β-CD at 283 and 298 K using atomistic molecular dynamics (MD) simulations.[15] It was observed that the affinities for the liquid/air interface of individual CD molecules and of small CD aggregates (<20 molecules) are negligible. On the other hand, the MD simulations in the bulk solution using up to 40 CD molecules showed that β-CD has a clear tendency to aggregate at 283 and 298 K, while for α-CD this tendency is clear at 283 K but less marked at 298 K. The study of the behavior of CD at interfaces is important because CD layers or films have been used as a main component of electrochemical and biological sensors,[16] having an important impact in the detection of pharmaceutical molecules like dextromethorphan,[17] ibuprofen,[18] diclofenac,[19] and volatile[20] or nitro aromatic compounds.[21] In these cases, the CDs interact with a large variety of guest molecules to form inclusion complexes and work as redox mediators. An important aspect in these devices is the formation of a CD film that is formed either by dip coating or by the self-assembly of a monolayer at the surface of the sensors. Presently, an open area of research is to study the effects on CD films of molecular organization, packing, and permeability on sensor performance.[22]

The aim of the present work is to describe comprehensively the spontaneous aggregation of α-CD in the bulk solution combined with the behavior at the liquid/air interface of the resulting aggregates. This is particularly interesting given that the driving forces for spontaneous aggregation in the bulk solution and the adsorption at a liquid/air interface are typically closely connected. We have carried out a characterization of the bulk aggregates of α-CD as a function of sample age, which is information that is lacking in the literature. Further, we have examined in detail the liquid/air interface, also as a function of sample age, to gain insight into the possible forces and mechanisms that determine and control the adsorption of α-CD aggregates. To reach these goals, we have employed a battery of experimental techniques: transmission electron microscopy, dynamic light scattering, dynamic surface tensiometry, Brewster angle microscopy, neutron reflectometry, and ellipsometry.

2. EXPERIMENTAL SECTION

2.1. Sample Preparation. Ultra pure water with a conductivity of 18.2 MΩ cm was obtained from a Millipore system, and α-CD was purchased from Sigma-Aldrich (purity >98%). The water content of α-CD was 10% by weight, as determined by Karl Fischer titration. To guarantee complete solubilization of α-CD, prior to any measurement, samples were heated for 30 min at 323 K and sonicated at room temperature for 15 min in an ultrasonic bath at 40 kHz. All solutions were made directly at their final bulk concentration rather than by dilution of a concentrated stock solution. Turbidity tests using UV−vis spectroscopy showed that the CD molecules were completely dissolved. All liquid samples were pipetted from the bulk to the measurement dish to avoid the transfer of kinetically trapped material formed at the liquid/air interface during its creation.[23] The data in the main text were all measured at 283 K. Measurements were limited to 10 mM as a result of the solubility limit of α-CD at 283 K being 39 mM (extrapolated from the 293−323 K data in ref 24).

2.2. Transmission Electron Microscopy (TEM). TEM was performed using a Philips CM-12 transmission electron microscope equipped with a digital camera MEGA VIEW-II DOCU and operated at 120 kV with a magnification of 730 000× and a maximum resolution of approximately 0.5 nm. The sample was prepared by the negative-staining technique with 2% (w/v) phosphotungstic acid. A carbon Formvar-coated copper grid was placed into the solution for 1 min and into the sodium phosphotungstate for another minute, and then the grid was dried. A small amount of sample was pipetted onto a TEM grid and allowed to dry at room temperature (usually for 1−2 h). In between and thereafter, excess liquid was wicked away with filter paper. Observations were made in a bright field.

2.3. Dynamic Light Scattering (DLS). Samples for DLS measurements were filtered between 15 and 20 times through a 0.2 μm cellulose acetate membrane (Titan 2, SUN Sri, U.S.). Because the refractive index of the solution is highly sensitive to the α-CD concentration, we used this property to check if a significant amount of α-CD was lost during the filtration process. We found that the refractive index of the solution before and after filtration was the same to the fifth significant figure, which means that the amount of CD retained was negligible. The DLS measurements as a function of time were made at a back scattering angle of 173°. A Z-sizer Nano model ZS (Malvern Instruments, UK) was used to perform the measurements with an incident beam of λ = 633 nm (He−Ne, 4.0 mW). Prior to being measured, samples were equilibrated inside the DLS cell for 20 min. Measurements consisted of at least 15 scans of 20−25 s. For the first 10 h, measurements were performed every 15 min. After that and up to 24 h, measurements were performed every 30 min. Thereafter, the same sample was followed for up to 300 h, measuring at different total times. All measurements were performed in triplicate. A "dust filter" option in the software was used to eliminate scans with a large number of counts. The electric field time correlation exponential function was solved for the translational diffusion coefficient using the Non Negative Least Square (CONTIN algorithm) method, which is reported as ideal for heterodisperse, polydisperse, and multimodal systems that cannot be resolved with the cumulant method.[25] Employing the Stokes−Einstein equation, we estimated the hydrodynamic effective sphere radius R_h while making the assumption that the aggregates formed are spherical.

2.4. Dynamic Surface Tensiometry (DST). The dynamic surface tension was measured using an image drop profile tensiometer (OCA20, Dataphysics, Germany) with a high-resolution USB camera (max 123 images/s sample rate) and a home-designed cell constructed with optic glass by Hellma, Germany. This cell allows measurements of up to 24 h at constant temperature and with low evaporation rate. Drops of 24 μL were created at 0.5 μL/s at the end of a syringe tip (1.650 mm outer diameter). Images of drop profiles were collected every minute. The surface tension γ was obtained using the Young−Laplace equation $\Delta P = (\rho_d - \rho_l)gh = (\gamma/R_1) + (\gamma/R_2)$, where ΔP is the pressure difference across the interface, ρ_d and ρ_l are the densities of the denser and the lighter phases, respectively, g is the gravitational constant, h is the height of the drop, and R_1 and R_2 are the two main drop curvature radius. Two different aqueous α-CD solutions were used: one was employed immediately after preparation, and the other was kept for 7 days at room temperature prior to being examined. The DST and BAM experiments were performed simultaneously using the same sample.

2.5. Brewster Angle Microscopy (BAM). Morphological information on the α-CD present at the liquid/air interface was obtained using BAM. A MicroBAM (KSV Instruments, Finland) machine equipped with a laser beam fixed to 53° for a water/air interface and a camera with a field of view of 3.6 mm × 4 mm and spatial resolution of 6 μm per pixel was used. Samples were placed in a Langmuir trough (Minimicro, KSV Instruments, Finland) of 98 cm^2 area, 57 mL subphase volume, with two movable barriers and a platinum rod sensor as a tensiometer (0.01−1 mN/m resolution), all in a dust-free environment. Three different aqueous α-CD solutions

DOI: 10.1021/acs.langmuir.6b01646
Langmuir 2016, 32, 6682−6690

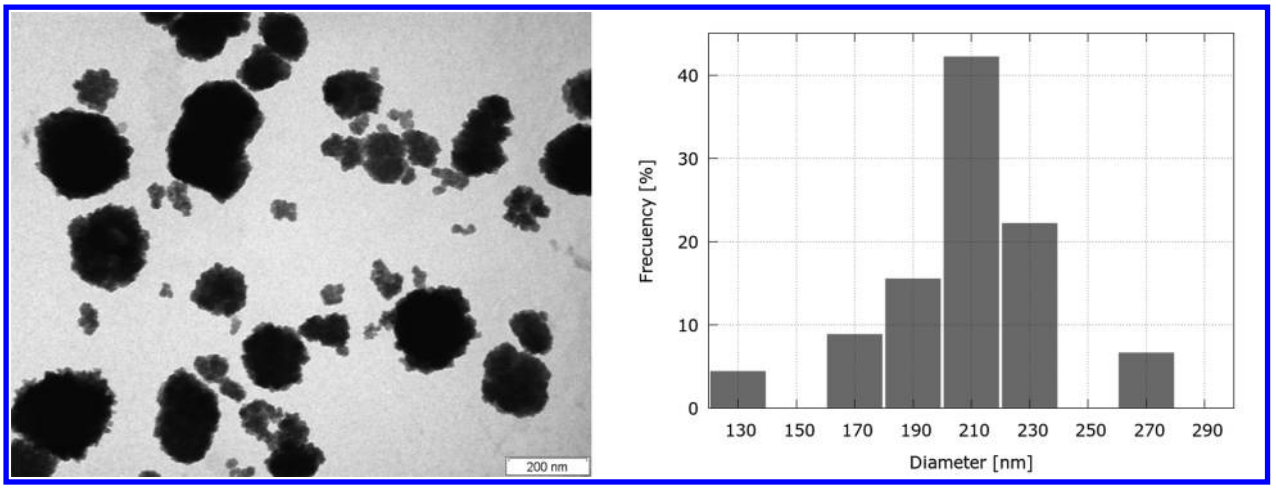

Figure 1. TEM micrographs of α-CD aggregates in a freshly prepared 10 mM solution at 283 K (left). This image was chosen to be as representative of the bulk samples measured as possible. Size distribution of the α-CD aggregates (right).

were used: two were employed immediately after preparation, and the third was kept for 7 days at room temperature prior to being examined. Before each experiment, the trough was cleaned with high purity chloroform and ultra pure water. The trough was considered clean when the water/air interface had a surface pressure of $\Pi < 0.2$ mN/m during the total compression of the surface with the movable barriers. After this, the water subphase was exchanged for the aqueous α-CD solution. BAM images were obtained in intervals of 15−30 min during the first 6 h and 30−60 min for the rest of the experiment, which typically lasted 20 h.

2.6. Neutron Reflectometry (NR). NR experiments were performed on the time-of-flight reflectometer FIGARO at the Institut Laue-Langevin (Grenoble, France).[26] Profiles of the neutron reflectivity R at the liquid/air interface as a function of the momentum transfer $q = 4\pi \sin(\theta)/\lambda$ were recorded using pulses in the wavelength range $\lambda = 2$−30 Å and at fixed incident angles of $\theta = 0.62°$ and 3.8°. The principles of the technique have been described elsewhere.[27] α-CD solutions were prepared in two different isotopic contrasts: D_2O and air contrast matched water (ACMW; a mixture of 8.1% by volume of D_2O in H_2O). NMR experiments in D_2O and in ACMW (performed in our laboratories) revealed that α-CD experiences a H → D replacement of three hydrogen atoms per glucopyranoside ring (presumably the hydroxyl groups). Thus, the scattering lengths of α-CD were calculated to be 376.31 fm in D_2O and 204.09 fm in ACMW. The value employed for the molecular volume of α-CD (995 Å^3) was determined by interpolating data in the literature.[28] The experimental scattering length density (ρ) obtained for D_2O was 6.24×10^{-6} Å^{-2}, while the values calculated for α-CD were 3.78×10^{-6} Å^{-2} in D_2O and 2.05×10^{-6} Å^{-2} in ACMW. The analysis of the NR data was performed using the homemade SANGRA software,[29] which is based on the implementation of the Parratt method[30] for the modeling of stratified layers by using the Fresnel equations. Also implemented in this software is the ability to model domains of different composition with sizes above the coherence length, which varies from hundreds of micrometers at low q (dominating the surface excess) to 1−10 μm at high q (dominating the structural analysis).[31]

Two types of analysis were carried out. First, data recorded over the full q-range in both isotopic contrasts were fitted using both a homogeneous layer model (i.e., reflection from the average scattering properties of the domains and gaps) and a heterogeneous layer model (i.e., additive reflection from the scattering of both the domains and the gaps weighted to their area coverage). Second, kinetic data were recorded in just one isotopic contrast (in ACMW) over a restricted q-range (up to 0.06 Å^{-1}). The product of the constrained ρ and the fitted thickness (τ) and volume fraction (v_f) of the layer was employed to calculate directly the surface excess using $\Gamma = \rho\tau v_f/(N_A b)$, where N_A is Avogadro's number and $b = \Sigma b_i$ is the coherent scattering length obtained from the sum of the corresponding values over all nuclei. The data were restricted to a low-q value of 0.03 Å^{-1} to be as independent as possible of details of the structural model applied.[32,33]

2.7. Ellipsometry (EP). EP data were recorded using a Picometer Light ellipsometer (Beaglehole Instruments, New Zealand) in the Partnership for Soft Condensed Matter (Grenoble, France) using a HeNe laser with $\lambda = 633$ nm and $\theta = 50°$. Measurements are of the change in polarization of light upon reflection at a surface, where the attenuation, Ψ, and phase shift, Δ, depend on the optical properties of the surface and on θ.[34] At the air/water interface, Ψ is insensitive to the optical properties of thin transparent films, so we model the measured parameter $\Delta_{surf} = \Delta - \Delta_0$, where Δ_{surf} is the change in Δ from the α-CD aggregates at the interface, Δ is the measured value, and Δ_0 is the value for pure water; its subtraction is to minimize effects on the data from surface roughness.[35]

An optical matrix model can be used to model the relation between Γ and Δ_{surf}. The complexities of such modeling are well documented,[36] and a comparison with data measured directly using NR is often used.[37] Even so, for the calibration of the ellipsometry data, in the thin film limit, a model with an oil-like layer (constant density; changing thickness) results in a linear $\Gamma(\Delta_{surf})$, and a model with a particle-like layer (constant thickness; changing density) results in a quadratic $\Gamma(\Delta_{surf})$.[38] A description of these models is given in part 1 of the Supporting Information. Their comparison produced very similar results, and the latter was chosen as more physically relevant for aggregate adsorption. As α-CD aggregates were shown to form layers with a thickness of 3.9 nm at the air−water interface using NR (see the Results and Discussion), a model of constant layer thickness with the following empirical relation was used: $\Gamma = (0.958 \times \Delta_{surf}) - (0.0348 \times \Delta_{surf}^2)$. The other main input parameter was the measured refractive index increment of α-CD (0.186 cm^3/g), which resulted in a "pure layer" refractive index of 1.462 (see part 2 of the Supporting Information). Two aqueous α-CD solutions were measured: one immediately after preparation (freshly mixed), and the other was aged in a refrigerator at 277 K for 9 days.

3. RESULTS AND DISCUSSION

3.1. α-Cyclodextrin Aggregates in the Bulk Aqueous Solution. A freshly prepared 10 mM α-CD bulk solution at 283 K was measured using TEM to determine if aggregates were present. Figure 1 shows a micrograph and the corresponding distribution histogram of the size of the aggregates after filtration through membranes with pores of 0.2 μm; note that samples filtered through 0.45 μm membranes like those used in the DLS measurements were also measured and showed no statistical differences. The image shows a uniform distribution of aggregates that are well separated from

DOI: 10.1021/acs.langmuir.6b01646
Langmuir 2016, 32, 6682−6690

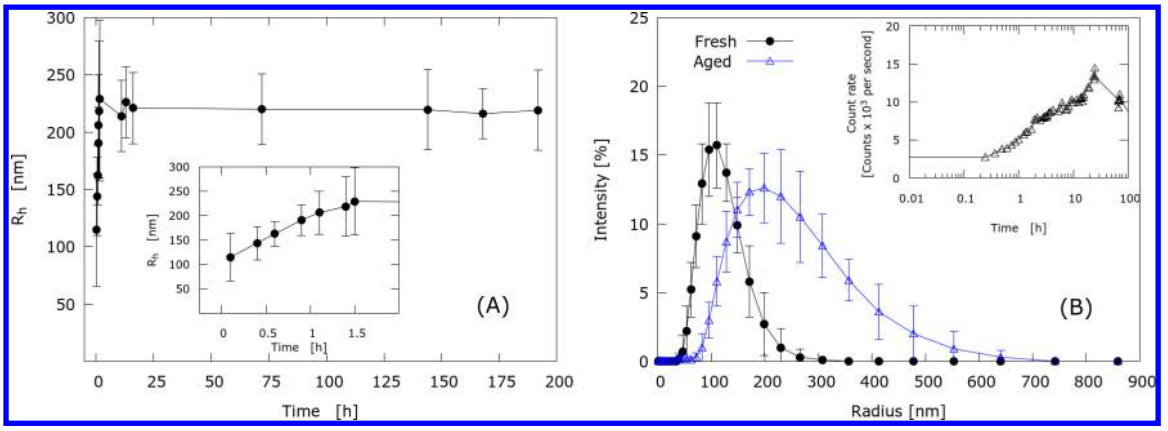

Figure 2. DLS measurements of (A) the hydrodynamic radius R_h of α-CD aggregates at 283 K as a function of time for 10 mM aqueous α-CD solutions filtered through a 0.2-μm cellulose membrane. The inset shows R_h for the first 2 h of measurement. (B) Size distribution of α-CD aggregates as a function of time and sample age. The aged sample was kept at 277 K for 8 days. The size distributions are reproducible as shown in part 3 of the Supporting Information for three fresh and independently prepared α-CD solutions. The inset shows the count rates as a function of time.

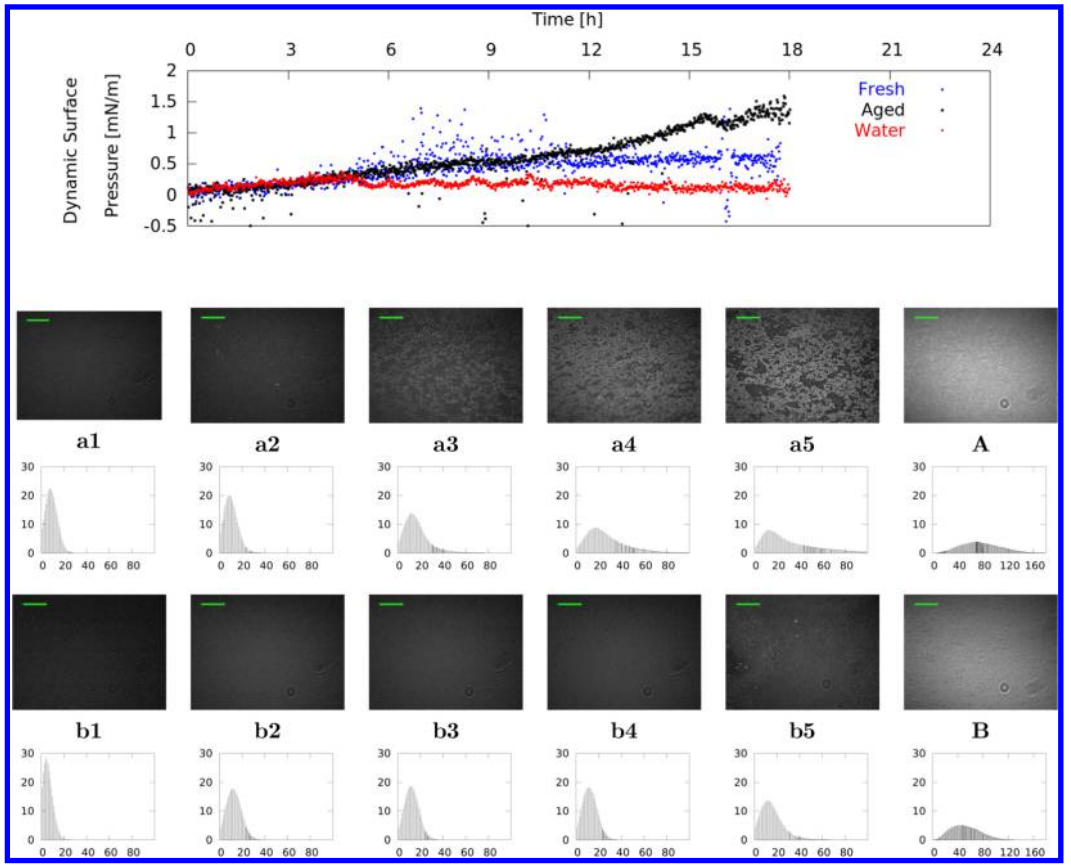

Figure 3. Dynamic surface pressure at 283 K for water and two 10 mM α-CD solutions: a freshly prepared sample and a sample that was aged for 7 days (kept at room temperature). Using the same samples, BAM images at different times were taken for the fresh (a) and aged (b) solutions. Numbers 1, 2, 3, 4, and 5 correspond to 0, 1, 3, 6, 20 h of elapsed time. The last observed surfaces, a5 and b5, were compressed in the Langmuir trough producing the images A and B, respectively. The horizontal green bars indicate the scale (800 μm). For each BAM image, the corresponding intensity histogram (pixels $\times$ 10^{-3} vs brightness) is shown.

each other, the distribution being relatively unimodal and symmetrical. Similar results using TEM have been also reported for β-CD.[39] Histograms of the average diameter area were generated from different TEM images of ~100 particles. The average diameter and uncertainties have been obtained from fitting histograms to single peak distributions giving 211 $\pm$ 24 nm.

The spontaneous formation of α-CD aggregates in solution was also followed with time using DLS to examine the size evolution of the resulting structures. Figure 2A indicates that large aggregates were present in the bulk solution already within a few minutes after filtration. As the two-dimensional TEM micrographs indicate circular structures, and as CDs without any encapsulated ligand are not expected to have a

DOI: 10.1021/acs.langmuir.6b01646
Langmuir 2016, 32, 6682−6690

dominant direction to grow because their structure is poorly defined,[40] the DLS data were analyzed assuming that the aggregates are spherical. The initial hydrodynamic radius (R_h) grows drastically from 110 to 230 nm within the first 10 h and then remains constant for 200 h. The slow initial aggregation kinetics corresponds to a gradual increase in the count rate (inset to Figure 2B). Figure 2B shows the size distribution of the aggregates for two different sample ages. The distribution is wider for the aged sample, which highlights the growth of aggregates in the first 10 h up to a maximum of 600 nm in size. Also, distributions are asymmetrical with a skewed shape toward larger areas, which increases with time. For β-CD, the aggregate size has also been found to increase with sample age.[41]

Note that measurements were also conducted using DLS for samples at 298 K (see part 3 of the Supporting Information). It was observed that the aggregates at 298 K both for the fresh and for the aged samples are smaller than at 283 K, with a smaller observed growth as a result of sample aging. The maxima of the size distributions are for the fresh samples 128 nm at 283 K and 82 nm at 298 K, while for the aged samples 171 nm at 283 K and 110 nm at 298 K. Further, measurements were also carried out at 283 K using isothermal titration calorimetry, but in this case the technique was insensitive to the presence of aggregates (see part 4 of the Supporting Information).

Assuming that α-CD molecules can be approximated to spheres with a diameter of 1 nm, and that the aggregates that form in solution are also spherical, we may estimate from the DLS data in Figure 2 that the number of molecules in the aggregates is on the order of $\sim 10^6-10^7$. The MD simulations recently performed for α-CD aggregates used only a maximum of 40 molecules,[15] and therefore inevitably they are not representative for the much larger aggregates determined experimentally in the present work. However, on the basis of the solvation free energy calculations, the latter computational work suggests that the driving forces for the formation of α-CD aggregates are the solute−solute interactions (mainly direct and water-mediated H-bonds between α-CD molecules), in contrast to the hydrophobic forces driving aggregation, for example, in surfactant micelles and also protein solutions.[42] This result is important in connection with the following sections of this work, focused on adsorption of the α-CD aggregates at the liquid/air interface.

3.2. α-Cyclodextrin Aggregates at the Liquid/Air Interface. Simultaneous DST and BAM measurements were carried out at 283 K on the same fresh and aged samples of 10 mM α-CD. We will present the tensiometry results in terms of the dynamic surface pressure to highlight the small changes observed, which are attributed to changes in the surface rather than bulk properties associated with α-CD solvation because the differences in the data from pure water increase with time, and from DLS the maximum monomer concentration would be expected at $t = 0$. In Figure 3, the value of the dynamic surface pressure increases for the freshly prepared sample. It has been commonly reported that α-CD is not surface active on the basis that its solutions do not result in a significant change in the surface tension as compared to that of pure water.[13,43] Nevertheless, the changes in dynamic surface pressure observed here, while small, are reproducible (see Figure S4 in part 5 of the Supporting Information) and statistically significant, and there is a further indication of the surface activity in α-CD samples by the small negative slope in the surface tension isotherm with respect to the bulk concentration (see Figure S5 in part 5 of the Supporting Information).

In the interpretation of the BAM images, white regions can be attributed to patches of material with sufficient optical contrast to be detected (e.g., high molecular density or anisotropy), while black regions indicate either gaps or areas of low molecular density or disordered material.[44−46] In the case of freshly prepared samples, BAM images and their corresponding intensity histograms in Figure 3 show the progressive formation of an interfacial layer with lateral inhomogeneities on the micrometer scale, consistent with that reported by ourselves previously.[14] At the start of the experiment (image a1), a very small amount of material is observed at the interface. After 1 and 3 h (images a2 and a3, respectively), α-CD domains are visible, albeit with a low intensity. These domains appear randomly dispersed at the interface leaving extended regions (in black) either with no material at the interface or with material present in a very low density or a disordered morphology. After 6 and 20 h (images a4 and a5, respectively), progressively more material populates the surface, and the morphology becomes more homogeneous with higher area coverage of the α-CD condensed domains.

To gain insight into the mechanism by which α-CD interacts with the water/air interface, now we compare the results from fresh and aged samples. The results for the aged sample (images b1 to b5) in Figure 3 confirm that the accumulation of material at the liquid/air interface is slower in this case. Only after 20 h (b5 in Figure 3) is it possible to identify clearly material at the interface in the BAM images.

It is interesting that when the last observed surface (images a5 and b5) was compressed in the Langmuir trough, the accumulated material at the surface is even clearer (images A and B). These results show that the interfacial layers created are not in fast dynamic equilibrium with the subphase, and that the resulting interfacial morphology exists in a kinetically trapped state. We may infer that the interface consists of domains of α-CD that are in a different phase to the adjoining gaps. As the α-CD domains grow larger with observation time, it follows that they are formed through the lateral coalescence of the material that has adsorbed to the interface. It is interesting to compare this interfacial morphology to that of spread films of human serum albumin, where it was recently shown that an extended network structure can also result in samples with very high surface tension values.[38] Such morphologies were also observed at the liquid/air interface of champagne.[47]

The different interfacial behavior of the aged α-CD samples must be attributed to the changes that take place in the bulk. Indeed it follows that slower diffusion of the larger bulk aggregates with time results in a slower interaction with the interface. We may conclude that the α-CD domains that form at the liquid/air interface arise primarily from the adsorption of the relatively small aggregates from the bulk (close to 100 nm radius) followed by their lateral coalescence and possibly by incorporation of α-CD monomers from the bulk to the aggregate to form more extended structures. The driving forces for this coalescence are attributed to solute−solute interactions, as suggested by the reported MD simulations.[15] However, the modest rise in dynamic surface pressure is slightly higher for the aged sample than for the fresh sample, although this may be related to the kinetically trapped nature of the formed layer. Additional techniques are required to elaborate this issue, so we went on to apply NR and EP to the same systems.

DOI: 10.1021/acs.langmuir.6b01646
Langmuir 2016, 32, 6682−6690

NR measurements were carried out on freshly prepared samples with a surface age of 7−8 h in ACMW and D_2O. The limited amount of information in the data limits the structural model applied to a single interfacial layer. The coherence length of the measurement falls in the micrometer range at the higher q values that dominate the structural analysis.[31] As the features observed in the BAM images span such length scales (Figure 3), it was not apparent to us whether it is more appropriate to apply a homogeneous or heterogeneous layer model (as described in the Experimental Section). As such, both models were applied to the experiment data, and the refined simultaneous fits are shown in red and blue, respectively, in Figure 4 with the relevant structural parameters and results listed in Table 1.

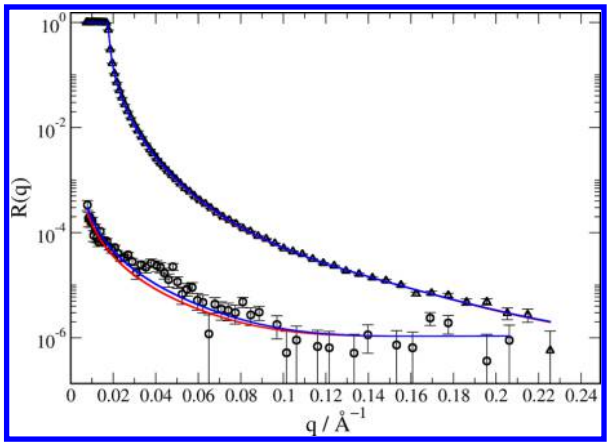

Figure 4. Experimental neutron reflectivity profiles obtained for a 10 mM α-CD solution at 283 K in D_2O (triangles) and in ACMW (circles). The blue lines are the fits using the homogeneous layer model, and the red lines are the fits using the heterogeneous layer model. Both fits practically coincide for the measurement in D_2O, and hence the red curve is barely visible.

Table 1. Structural Parameters and Results from the Application of Homogeneous and Heterogeneous Layer Model Fits to the NR Data at 283 K Shown in Figure 4

parameter/result	homogeneous model	heterogeneous model
thickness (nm)	3.95	3.87
area coverage of domain 1[a]	1 (fixed)	0.169
fraction of α-CD in domain 1[a]	0.119	0.652
standard deviation	24.2	23.7
surface excess (mg/m^2)	0.80	0.72

[a]Domain 1 is the proportion of the interface coverage by α-CD aggregates as indicated by the BAM images; other parameters are layer roughnesses = 2.5 Å; D_2O residual background = 5.1×10^{-7} (fitted from pure air/D_2O data); ACMW residual background = 1.1×10^{-6} (fitted from the last 8 points of the ACMW data in Figure 4).

A layer thickness of 3.9 nm is determined from the application of both models to the experimental data. Given that the longest axis of the molecule is approximately 1 nm, we may infer that the interfacial morphology extends beyond a monolayer of α-CD monomers, as it has been reported for systems composed by β-CD and lipid monolayers.[48] It is interesting to place the nanometer-scale film thickness determined using NR in the context of work dealing with aggregates created in systems involving α-CD with inclusion hosts. For example, in the work by Polarz et al., silica was used to template worm-like aggregates of α-CD in the presence of xylene, and TEM images showed an aggregate−aggregate separation on the order of several nanometers.[49] In the present work, α-CD was not complexed to an inclusion host, but the film created was nevertheless templated, by a planar hydrophobic boundary between liquid and air. It will be interesting in the future to resolve and compare the driving forces for the templating in the two different types of systems with a view to optimization of film formation.

In the case of the heterogeneous layer model, the proportion of α-CD in the domains is 17%; note that forcing this value to be higher resulted in worse fits to the experimental data. This is the only information about the possible composition of the domains we have resolved to date. There are very similar values for the surface excess (a difference of 10%) and the standard deviation (difference of 2%) from the two models, which has two implications. First, they show that we cannot interpret any more information about the interfacial structure from these data beyond that specified above. Second, they show that it is reasonable to apply either model to determine the surface excess during adsorption, for which we recorded kinetic data only in ACMW and up to q = 0.06 Å^{-1}. As such, with a fixed domain composition of 17% α-CD to limit the number of fitting parameters, this model was applied to the kinetic data for comparison with ellipsometry (EP) measurements.

Figure 5 shows a comparison of the NR and EP data of fresh samples over several hours. The surface excesses measured

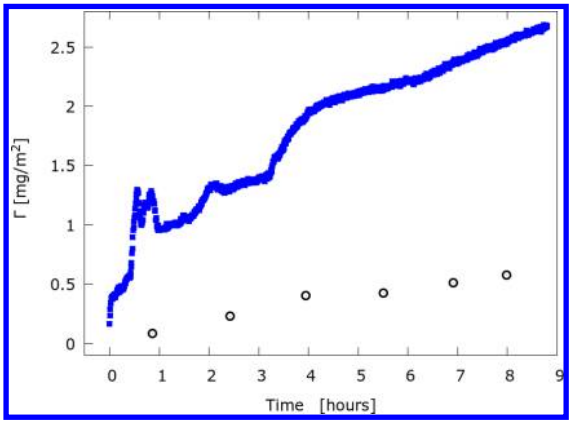

Figure 5. Kinetic evolution of the surface excess for 10 mM α-CD solutions at 283 K measured using NR (○) and EP (blue ■).

using EP are higher by about a factor of 5. If the adsorbed layer were in a fast dynamic equilibrium with the subphase (e.g., a soluble surfactant at sufficient bulk concentration), such a discrepancy could be explained by anisotropy (i.e., different refractive indices parallel with and perpendicular to the interface); note that the microscopic heterogenity of the interface is not a consideration here given that the coherence length of the EP measurement is much larger than the domain size.[31] However, anisotropy of a factor of 5 would be double that observed even of highly ordered domains in lipid-based systems that exhibit lateral phase separation,[44] and in the absence of inclusion hosts the structure of α-CD aggregates may be expected to be rather poorly defined.[40] An alternative explanation, given the nonequilibrium nature of the kinetically trapped films created here, is that the different geometries and materials of the sample containers used in the NR and EP

DOI: 10.1021/acs.langmuir.6b01646
Langmuir 2016, 32, 6682−6690

measurements resulted in different adsorption rates: the former vessels were shallower and were made of a hydrophobic material to which deposition of aggregates may have occurred. As such, we go ahead now to exploit the precision, sensitivity, and time resolution of EP with a comparison of the effects of sample age on the adsorption kinetics using the isotropic optical model to calculate Γ, yet with a degree of caution we restrict our interpretations to relative changes rather than the absolute scaling.

Figure 6 shows the surface excess evolution of fresh and aged α-CD solutions. The EP data of the freshly prepared solution

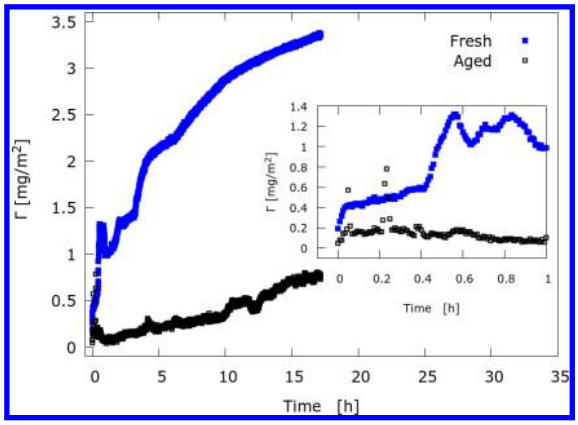

Figure 6. Kinetic evolution of the surface excess at 283 K for fresh and aged 10 mM α-CD solutions measured using EP. The aged sample was kept at 277 K for 9 days. The inset shows the surface excess during the first hour of measurement.

show clearly a slow but continual increase in the surface excess with time, consistent with the accumulation of material at the interface observed using BAM. The fact that there are temporal fluctuations in the measured values suggests the formation of a nonuniform layer on the micrometer scale, with condensed domains of the aggregates in coexistence with less dense areas or gaps, as is also supported by BAM and considered in the NR fittings (the heterogeneous model). In the case of EP, the temporal fluctuations may be attributed to the lateral movement of the domains in and out of the region probed by the laser as a result of Brownian motion, as has been seen, for example, in mixtures that exhibit phase separation.[23,47] It is interesting that an interfacial excess plateau was not found within the observation time. This feature suggests that the adsorption and coalescence processes of the aggregates would probably take days or longer to reach equilibrium while the gaps at the interface are being slowly filled.

The EP data show a drastic reduction in the surface excess kinetics for the aged sample as compared to the fresh sample, providing further evidence for the observations made about the adsorption and subsequent coalescence at the interface of aggregates that had formed in the bulk on the basis of the BAM images above. Indeed the fact that the adsorption is so much slower for the aged solutions, yet the bulk monomer concentration had probably remained practically constant, indicates strongly that the dominant interfacial interactions are from the aggregates, and the adsorption of monomers is unfavorable. This inference supports the conclusions made in our recent study based on MD simulations.[15] Even so, the adsorption of monomers to the condensed α-CD domains is not precluded and is a matter that merits further investigation. Again, the temporal fluctuations show that the interface is laterally inhomogeneous on the micrometer scale. The physical picture indicated by BAM and EP can be put into context of the DLS data for fresh versus aged samples (Figure 2) where larger α-CD aggregates were found in the bulk solution with time and that, by Brownian diffusion, would take longer times to reach the liquid/air interface. Hence, we may conclude that the smaller aggregates can adsorb at a faster rate and then flocculate laterally for the freshly mixed samples, producing the large domains seen using BAM at faster rate.

Note that measurements were also carried out at 298 K using ellipsometry (see part 6 of the Supporting Information). In this case, there was only a small effect on the adsorption rate, but reduced temporal fluctuations showed that the films were more uniform on the micrometer scale. This finding shows that temperature is a key variable in film formation and as such is a promising candidate to tune in future investigations.

4. CONCLUDING REMARKS

Through exploitation of an extended set of bulk and surface techniques, a systematic study of α-CD aqueous solutions has been performed. The formation of α-CD aggregates in the bulk and the consequent formation at the liquid/air interface of α-CD domains with lateral inhomogeneities on the micrometer-scale have been characterized. The main results can be summarized as follows: (i) α-CD molecules spontaneously aggregate in the bulk solution, (ii) the average size of these aggregates increases with time, (iii) through a diffusion mechanism α-CD aggregates progressively adsorb to the interface over many hours resulting in only minor changes in the dynamic surface pressure, the process being even slower for aged samples, which is attributed to the slower diffusion of the larger aggregates, and (iv) once at the interface, the α-CD aggregates form, through lateral coalescence, extended domains on the micrometer scale in a kinetically trapped film with a thickness on the nanometer scale.

A particularly significant observation is the drastic reduction in adsorption for aged solutions, even though the bulk monomer concentration had remained practically constant during the intervening period. This result provides strong experimental indications that (1) the material at the interface is dominated by the adsorption of α-CD aggregates that had formed in the bulk and (2) the adsorption of α-CD monomers at a bare liquid/air interface is unfavorable.

At a microscopic level, the ability of the very flexible α-CD molecules to form many α-CD/α-CD and α-CD/water H-bonds suggests that the driving force for their aggregation in the bulk solution and for their flocculation once at the interface is the solute−solute interactions, as recently indicated from MD simulation studies. Our results therefore highlight the complexity of the parallel physical processes taking place on the measured time scales in the binary system composed only of α-CD molecules and water. Although this would initially seem like a simple system, we have resolved a complex variety of processes.

The spontaneous formation of α-CD aggregates in the bulk and their transport to the interface with a minimal change in its free energy opens interesting avenues for applied research. The present work shows that for α-CD aqueous solutions, sample age is a key parameter to tune their bulk and interfacial properties. This characteristic could, for example, be exploited for delivery applications in a range of systems: in the bulk to improve and control the solubilization of poorly soluble drugs,

DOI: 10.1021/acs.langmuir.6b01646
Langmuir 2016, 32, 6682−6690

and at the surface to optimize the performance and design of biosensors.

■ ASSOCIATED CONTENT

Supporting Information

The Supporting Information is available free of charge on the ACS Publications website at DOI: 10.1021/acs.langmuir.6b01646.

(1) Ellipsometry: additional details on the data analysis, (2) refractive index measurements: experimental details and results, (3) dynamic light scattering: additional results, (4) isothermal titration calorimetry: experimental details and results, (5) dynamic surface tensiometry: additional results, and (6) ellipsometry: additional results (PDF)

■ AUTHOR INFORMATION

Corresponding Authors

*E-mail: campbell@ill.eu.

*E-mail: jcampos@correo.cua.uam.mx.

*E-mail: costasmi@unam.mx.

Present Address

⊥Laboratorio de Nanobiotecnología, Facultad de Ciencias Químicas y Farmacéuticas, Universidad de Chile, Santiago 8320000, Chile.

Notes

The authors declare no competing financial interest.

■ ACKNOWLEDGMENTS

We are grateful to Nuria Esturau for performing the NMR experiments and to Simon Wood for his technical assistance. We thank the Institut Laue-Langevin (ILL, Grenoble, France) for beam time on FIGARO and the Partnership for Soft Condensed Matter for the use of the ellipsometer. J.H.-P. thanks CONACyT-México for a graduate student scholarship. N.H. acknowledges funding from Programa Fondecyt Postdoctoral number 3140489. J.C.-T., J.H.-P, and M.C. thank the Red Temática Materia Condensada Blanda (Mexico) for travel and living expenses to ILL. This work was supported by MINECO-Spain (grant MAT2011-25501) to Á.P., CONACyT-México grant numbers CB-2012/182526 to J.C.-T. and 099844 to M.C., and PAIP-FQ-UNAM grant number 5000-9018 to M.C.

■ REFERENCES

(1) Connors, K. A. The Stability of Cyclodextrin Complexes in Solution. *Chem. Rev.* **1997**, *97* (5), 1325−1357.

(2) Szejtli, J. Introduction and General Overview of Cyclodextrin Chemistry. *Chem. Rev.* **1998**, *98* (97), 1743−1753.

(3) Easton, C. J.; Lincoln, S. F. *Modified Cyclodextrins: Scaffolds and Templates for Supramolecular Chemistry*; Imperial College Press: London, 1999.

(4) Challa, R.; Ahuja, A.; Ali, J.; Khar, R. K. Cyclodextrins in Drug Delivery: An Updated Review. *AAPS PharmSciTech* **2005**, *6* (2), E329−E357.

(5) Coleman, A. W.; Nicolis, I.; Keller, N.; Dalbiez, J. P. Aggregation of Cyclodextrins: An Explanation of the Abnormal Solubility of β-Cyclodextrin. *J. Inclusion Phenom. Mol. Recognit. Chem.* **1992**, *13* (2), 139−143.

(6) González-Gaitano, G.; Rodríguez, P.; Isasi, J. R.; Fuentes, M.; Tardajos, G.; Sánchez, M. The Aggregation of Cyclodextrins as Studied by Photon Correlation Spectroscopy. *J. Inclusion Phenom. Mol. Recognit. Chem.* **2002**, *44* (1−4), 101−105.

(7) Puskás, I.; Schrott, M.; Malanga, M.; Szente, L. Characterization and Control of the Aggregation Behavior of Cyclodextrins. *J. Inclusion Phenom. Mol. Recognit. Chem.* **2013**, *75* (3−4), 269−276.

(8) Valente, A. J. M.; Carvalho, R. A.; Söderman, O. Do Cyclodextrins Aggregate in Water? Insights from NMR Experiments. *Langmuir* **2015**, *31* (23), 6314−6320.

(9) Messner, M.; Kurkov, S. V.; Flavià-Piera, R.; Brewster, M. E.; Loftsson, T. Self-Assembly of Cyclodextrins: The Effect of the Guest Molecule. *Int. J. Pharm.* **2011**, *408* (1−2), 235−247.

(10) He, Y.; Fu, P.; Shen, X.; Gao, H. Cyclodextrin-Based Aggregates and Characterization by Microscopy. *Micron* **2008**, *39* (5), 495−516.

(11) Messner, M.; Kurkov, S. V.; Jansook, P.; Loftsson, T. Self-Assembled Cyclodextrin Aggregates and Nanoparticles. *Int. J. Pharm.* **2010**, *387* (1−2), 199−208.

(12) Ferreira, M.; Bricout, H.; Azaroual, N.; Landy, D.; Tilloy, S.; Hapiot, F.; Monflier, E. Cyclodextrin/Amphiphilic Phosphane Mixed Systems and Their Applications in Aqueous Organometallic Catalysis. *Adv. Synth. Catal.* **2012**, *354* (7), 1337−1346.

(13) Hernández-Pascacio, J.; Banquy, X.; Pérez-Casas, S.; Costas, M.; Amigo, A.; Piñeiro, Á. A Small Molecular Size System Giving Unexpected Surface Effects: α-Cyclodextrin + Sodium Dodecyl Sulfate in Water. *J. Colloid Interface Sci.* **2008**, *328* (2), 391−395.

(14) Hernández-Pascacio, J.; Garza, C.; Banquy, X.; Díaz-Vergara, N.; Amigo, A.; Ramos, S.; Castillo, R.; Costas, M.; Piñeiro, Á. Cyclodextrin-Based Self-Assembled Nanotubes at the Water/Air Interface. *J. Phys. Chem. B* **2007**, *111* (44), 12625−12630.

(15) Mixcoha, E.; Campos-Terán, J.; Piñeiro, Á. Surface Adsorption and Bulk Aggregation of Cyclodextrins by Computational Molecular Dynamics Simulations as a Function of Temperature: α-CD vs β-CD. *J. Phys. Chem. B* **2014**, *118* (25), 6999−7011.

(16) Luong, J. H.; Brown, R. S.; Male, K. B.; Cattaneo, M. V.; Zhao, S. Enzyme Reactions in the Presence of Cyclodextrins: Biosensors and Enzyme Assays. *Trends Biotechnol.* **1995**, *13* (11), 457−463.

(17) Khaled, E.; Kamel, M. S.; Hassan, H. N. a.; Aboul-Enein, H. Y. Cyclodextrin-Based Dextromethorphan Potentiometric Sensors. *J. Electroanal. Chem.* **2011**, *661* (1), 239−244.

(18) Sousa, T. F. A.; Amorim, C. G.; Montenegro, M. C. B. S. M.; Araújo, A. N. Cyclodextrin Based Potentiometric Sensor for Determination of Ibuprofen in Pharmaceuticals and Waters. *Sens. Actuators, B* **2013**, *176*, 660−666.

(19) Lenik, J. A New Potentiometric Electrode Incorporating Functionalized β-Cyclodextrins for Diclofenac Determination. *Mater. Sci. Eng., C* **2014**, *45*, 109−116.

(20) Girschikofsky, M.; Rosenberger, M.; Belle, S.; Brutschy, M.; Waldvogel, S. R.; Hellmann, R. Alkylated Cyclodextrins as Effective Affinity Materials in Chemical Sensing of Volatile Aromatic Hydrocarbons Using an Optical Planar Bragg Grating Sensor. *Anal. Chim. Acta* **2013**, *791*, 51−59.

(21) Tredici, I.; Merli, D.; Zavarise, F.; Profumo, A. α-Cyclodextrins Chemically Modified Gold Electrode for the Determination of Nitroaromatic Compounds. *J. Electroanal. Chem.* **2010**, *645* (1), 22−27.

(22) Ogoshi, T.; Harada, A. Chemical Sensors Based on Cyclodextrin Derivatives. *Sensors* **2008**, *8* (8), 4961−4982.

(23) Campbell, R. A.; Yanez Arteta, M.; Angus-Smyth, A.; Nylander, T.; Noskov, B. A.; Varga, I. Direct Impact of Nonequilibrium Aggregates on the Structure and Morphology of Pdadmac/SDS Layers at the Air/Water Interface. *Langmuir* **2014**, *30* (29), 8664−8674.

(24) Frömming, K. H.; Szejtli, J. *Cyclodextrins in Pharmacy*; Academic Publishers: The Netherlands, 1994; p 10.

(25) Scotti, A.; Liu, W.; Hyatt, J. S.; Herman, E. S.; Choi, H. S.; Kim, J. W.; Lyon, L. A.; Gasser, U.; Fernandez-Nieves, A. The CONTIN Algorithm and Its Application to Determine the Size Distribution of Microgel Suspensions. *J. Chem. Phys.* **2015**, *142* (23), 234905.

(26) Campbell, R. A.; Wacklin, H. P.; Sutton, I.; Cubitt, R.; Fragneto, G. FIGARO: The New Horizontal Neutron Reflectometer at the ILL. *Eur. Phys. J. Plus* **2011**, *126* (11), 107.

DOI: 10.1021/acs.langmuir.6b01646
Langmuir 2016, 32, 6682−6690

(27) Lu, J. R.; Thomas, R. K.; Penfold, J. Surfactant Layers at the Air/water Interface: Structure and Composition. *Adv. Colloid Interface Sci.* **2000**, *84* (1−3), 143−304.
(28) Origlia-Luster, M. L.; Call, T. G.; Woolley, E. M. Apparent Molar Volumes and Apparent Molar Heat Capacities of Aqueous Solutions of α- and β-Cyclodextrins at Temperatures from 278.15 to 393.15 K and at the Pressure 0.35 MPa. *J. Chem. Thermodyn.* **2001**, *33* (11), 1587−1596.
(29) Piñeiro, Á. http://smmb.usc.es./tools.html.
(30) Parratt, L. G. Surface Studies of Solids by Total Reflection of X-Rays. *Phys. Rev.* **1954**, *95* (2), 359−369.
(31) Lauter-Pasyuk, V. Neutron Grazing Incidence Technique for Nanoscience. *Collect. la Société Française la Neutron* **2007**, *7*, 221−240.
(32) Angus-Smyth, A.; Campbell, R. A.; Bain, C. D. Dynamic Adsorption of Weakly Interacting Polymer/Surfactant Mixtures at the Air/Water Interface. *Langmuir* **2012**, *28* (34), 12479−12492.
(33) Ábraham, Á.; Campbell, R. A.; Varga, I. New Method to Predict the Surface Tension of Complex Synthetic and Biological Polyelectrolyte/surfactant Mixtures. *Langmuir* **2013**, *29* (37), 11554−11559.
(34) Azzam, R. M. A.; Bashara, N. M. *Ellipsometry and Polarized Light*; North Holland: Amsterdam, 1997; pp 283−288.
(35) Langevin, D. *Light Scattering by Liquid Surfaces and Complementary Techniques (Surfactant Science)*; CRC Press: New York, 1992; pp 333−364.
(36) Li, P. X.; Thomas, R. K.; Penfold, J. Limitations in the Use of Surface Tension and the Gibbs Equation to Determine Surface Excesses of Cationic Surfactants. *Langmuir* **2014**, *30* (23), 6739−6747.
(37) Manning-Benson, S.; Parker, S. R. W.; Bain, C. D.; Penfold, J. Measurement of the Dynamic Surface Excess in an Overflowing Cylinder by Neutron Reflection. *Langmuir* **1998**, *14* (5), 990−996.
(38) Campbell, R. A.; Ang, J. C.; Sebastiani, F.; Tummino, A.; White, J. W. Spread Films of Human Serum Albumin at the Air−Water Interface: Optimization, Morphology, and Durability. *Langmuir* **2015**, *31* (50), 13535−13542.
(39) Bonini, M.; Rossi, S.; Karlsson, G.; Almgren, M.; Lo Nostro, P.; Baglioni, P. Self-Assembly of Beta-Cyclodextrin in Water. Part 1: Cryo-TEM and Dynamic and Static Light Scattering. *Langmuir* **2006**, *22* (4), 1478−1484.
(40) Dodziuk, H. Rigidity versus Flexibility. A Review of Experimental and Theoretical Studies Pertaining to the Cyclodextrin Nonrigidity. *J. Mol. Struct.* **2002**, *614* (1−3), 33−45.
(41) Sa Couto, A.; Loftsson, T. β-Cyclodextrin Aggregates: The Osmolarity Method in Comparison to Other Detection Methods; http://abstracts.aaps.org/Verify/AAPS2015/PosterSubmissions/T2269.pdf.
(42) Heintz, A.; Lehmann, J. K.; Kozlova, S. A.; Balantseva, E. V.; Bazyleva, A. B.; Ondo, D. Micelle Formation of Alkylimidazolium Ionic Liquids in Water and in Ethylammonium Nitrate Ionic Liquid: A Calorimetric Study. *Fluid Phase Equilib.* **2010**, *294* (1−2), 187−196.
(43) Piñeiro, Á.; Banquy, X.; Pérez-Casas, S.; Tovar, E.; García, A.; Villa, A.; Amigo, A.; Mark, A. E.; Costas, M. On the Characterization of Host−Guest Complexes: Surface Tension, Calorimetry, and Molecular Dynamics of Cyclodextrins with a Non-Ionic Surfactant. *J. Phys. Chem. B* **2007**, *111* (17), 4383−4392.
(44) Pérez-Morales, M.; Pedrosa, J. M.; Martín-Romero, M. T.; Möbius, D.; Camacho, L. Reversible Trilayer Formation at the Air−Water Interface from a Mixed Monolayer Containing a Cationic Lipid and an Anionic Porphyrin. *J. Phys. Chem. B* **2004**, *108* (14), 4457−4465.
(45) Cárdenas, M.; Nylander, T.; Jönsson, B.; Lindman, B. The Interaction between DNA and Cationic Lipid Films at the Air-Water Interface. *J. Colloid Interface Sci.* **2005**, *286* (1), 166−175.
(46) Stefaniu, C.; Brezesinski, G.; Möhwald, H. Polymer-Capped Magnetite Nanoparticles Change the 2D Structure of DPPC Model Membranes. *Soft Matter* **2012**, *8* (30), 7952−7959.
(47) Peron, N.; Meunier, J.; Cagna, A.; Valade, M.; Douillard, R. Phase Separation in Molecular Layers of Macromolecules at the Champagne-Air Interface. *J. Microsc.* **2004**, *214* (Pt 1), 89−98.
(48) Mascetti, J.; Castano, S.; Cavagnat, D.; Desbat, B. Organization of Beta-Cyclodextrin under Pure Cholesterol, DMPC, or DMPG and Mixed Cholesterol/phospholipid Monolayers. *Langmuir* **2008**, *24* (17), 9616−9622.
(49) Polarz, S.; Smarsly, B.; Bronstein, L.; Antonietti, M. From Cyclodextrin Assemblies to Porous Materials by Silica Templating. *Angew. Chem., Int. Ed.* **2001**, *40* (23), 4417.

DOI: 10.1021/acs.langmuir.6b01646
Langmuir 2016, 32, 6682−6690